Doi: 10.31276/VJSTE.61(2).29-34

Treatment of benzene, toluene, and xylene by deep oxidation on CuO catalytic materials synthesised from red mud and rice husk ash

Thanh Tinh Nguyen[1], Phung Anh Nguyen[2], Thi Thuy Van Nguyen[2], Tri Nguyen[2], Ky Phuong Ha Huynh[1*]

[1]Research Institute for Sustainable Energy, University of Technology, Vietnam National University, Ho Chi Minh city
[2]Institute of Chemical Technology, Vietnam Academy of Science and Technology

Received 5 October 2018; accepted 10 January 2019

Abstract:

In this study, CuO-doped material fabricated from rice husk ash and red mud was modified by CeO_2 promoter and urea using the impregnation method. The obtained samples were investigated for catalytic degradation of aromatic derivatives (benzene, toluene, and *p*-xylene - BTX) at a temperature range of 275 to 450°C. This demonstrated that all samples were highly active in the BTX treatment. Several techniques, such as X-ray powder diffraction analysis (XRD), scanning electron microscopy (SEM), transmission electron microscopy (TEM), BET surface areas and pore parameters (N_2 physisorption), and hydrogen temperature programed reduction (H_2-TPR), were applied to analyse properties of obtained materials. The modification of CuO-doped catalytic material by both CeO_2 promoter and urea resulted in decreased particle size, increased CuO dispersion, and improved catalytic activity of the material. In relation to this material, the conversions of benzene, toluene, and p-xylene were 66.1%, 96.8%, and 96.8% respectively at 375°C.

Keywords: **benzene, CuO-doped catalytic material, toluene, treatment, xylene.**

Classification numbers: **2.2, 2.3**

Introduction

The emission of volatile organic compounds (VOCs) due to industrial manufacturing has caused many severe environmental problems, such as petrochemical smog, acid rain, ozone layer depletion, and climate change [1]. Aromatic compounds, particularly benzene, toluene, and xylene (BTX), are used as raw materials in the production of chemicals as well as ordinary solvents [2]. Therefore, emissions of these pollutants require strict monitoring. Deep oxidation is a potential method of treating VOCs at low concentrations [3]. This does not require additional fuel, which enables the reduced consumption of energy; this method can also be applied at a lower temperature ($\leq 450^0$C) relative to thermal oxidation (700^0C) [4]. The exploitation of catalysts for deep oxidation based on waste materials has recently sparked interest because it is an environmentally friendly process which can not only reduce costs but also save raw materials.

Red mud (RM) refers to the residual solid waste which remains after bauxite leaching by alkali in the aluminum industry. Its primary components include Fe_2O_3, Al_2O_3, SiO_2, CaO, and Na_2O [5, 6]. Since it offers advantages such as small particle size, high thermal stability, sintering resistance, and resistance to poisoning, substantial efforts have been directed toward utilising RM as an adsorbent as well as a catalyst for environmentally benign processes [6, 7]. However, the catalytic application of RM is limited due to its high alkalinity, primarily originating from Na and Ca, which can poison and reduce catalytic activity [8]. Rice husk ash (RHA), which is composed of SiO_2 (95%), was released through a reuse RHA process for energy purposes. One idea has been considered to investigate the synthesis of material with a partial zeolite structure (ZRM) through the

*Corresponding author: Email: hkpha@hcmut.edu.vn

combination of RHA and RM with the primary components of Fe_2O_3, Al_2O_3, SiO_2, CaO, and Na_2O at high pH. The alkalinity must be neutralised or acidified, which can reduce the cost of this synthesis process. In the research of Quyen, et. al. [6], material in nanoparticles with a partial zeolite structure (ZRM) was synthesised successfully by using the waste materials from red mud (RM) containing alumina and alkalis, or NaOH and rice husk ash (RHA). Relative to RM (23.59 m^2/g) or RHA (28.35 m^2/g), catalysts with partial zeolite structure have significantly higher specific surface area (70.76 m^2/g) [6].

Furthermore, CuO-CeO_2 catalysts supported on ZRM were prepared through the co-impregnation method. The modification of the CuO and ZRM catalyst by adding CeO_2 had reduced the size and increased the dispersive performance, and the synchronism of catalysts' nanoparticles significantly improved the catalytic activity in *p*-xylene oxidation at 275 to 400^{0}C. Sample 5 wt.% CuO and ZRM modified with 3 wt.% CeO_2 (denoted as CuCe) was optimal for *p*-xylene deep oxidation. Furthermore, CuO and ZRM catalyst was also prepared through a urea-nitrate combustion technique. It demonstrated that through this technique, active sites such as copper and iron oxides had enhanced dispersion on material surfaces with smaller particle size, which increased the activity of catalysts in *p*-xylene oxidation. Catalyst 5 wt.% CuO and ZRM synthesised with the urea and nitrate molar ratio of 2 was optimal (denoted as Cu(U)). Therefore, the combination of adding CeO_2 and using the urea-nitrate combustion technique is expected to improve properties of material, resulting in an enhanced catalytic performance in the BTX oxidation. In this research, 5 wt.% CuO/ZRM material modified with 3 wt.% CeO_2 was synthesised through a urea-nitrate combustion method with the urea-nitrate molar ratio of 2 (denoted as CuCe(U)). The obtained catalyst and the optimal catalysts in our previous research (i.e., Cu(U) and CuCe samples) were investigated through BTX oxidation.

Experimental

Catalyst synthesis and characterisation

The material with partial zeolite structure (ZRM) was synthesised from red mud and rice husk based on the process detailed in the research [6], which involved $Cu(NO_3)_2.3H_2O$ (Xilong, >99%), $Ce(NO_3)_3.6H_2O$ (Merck, >99%), urea (Xilong, >99%), and deionised water. Cu(U) and ZRM as well as CuCe and ZRM catalysts were synthesised based on the process detailed in our previous research [9]. Catalysts were obtained through the wet impregnation of the mixture solution of $Cu(NO_3)_2$, and $Ce(NO_3)_3$ and urea on ZRM. The loading content of CuO and CeO_2 was fixed at 5 wt.% and 3 wt.%, respectively, and a urea-nitrate molar ratio of 2. The obtained suspension was dried in air at 80, 100, and 120^{0}C for 2 hours at each temperature. Finally, the sample was calcined in air flow at 500^{0}C for 3 hours. This sample was denoted as CuCe(U) and ZRM. The characteristics of the as-synthesised materials were determined using the distinct techniques presented in our paper [9].

Catalytic activity

Before the activity was tested, all samples were activated at 450^{0}C for 4 hours in air flow with a velocity of 200 $ml.min^{-1}$. The catalytic measurement of the samples in deep oxidation of BTX (benzene, toluene and p-xylene) was performed in a micro-flow reactor under atmospheric pressure at a temperature range of 275 to 450^{0}C. The concentrations of BTX and O_2 in the stream were 0.34 and 10.5 mol%, respectively. The weight hourly space velocity (WHSV) was 12,000 $ml.h^{-1}.g^{-1}$, and the mass of catalyst was 1.0 g with a size range of 0.25 to 0.50 mm.

Gas mixtures in the input and output flow of the reactor were analysed using the Agilent 6890 Plus Gas Chromatograph (HP-USA) with FID detector, capillary column DB 624 (outer diameter of 0.32 mm; thickness of 0.25 μm and length of 30 m). The tests were conducted in triplicate to ensure the accuracy of the results.

Results and discussion

Physicochemical characteristics of materials

X-ray powder diffraction (XRD) patterns of the samples were displayed in Fig. 1, which indicates the main components of red mud and rice husk ash; the typical reflections of hematite (Fe_2O_3) can be observed at 2θ = 24.4, 29.8, 34.5, 36.1, 41.3, 54.4, 63.5, and 64.5^0. According to Huang, et al. [7], the peaks of A-type zeolite can be observed at 2θ = 24.4, 29.8, and 36.1^0. Additionally, according to Volanti, et al. [10], the typical reflections of CuO can be exhibited at 2θ = 36.1, 41.3, 49.9, and 54.4^0 in the XRD patterns. Therefore, it demonstrated that the XRD patterns of the samples appeared simultaneously with the primary components of the red mud (hematite), A-type zeolite, and CuO crystals, with the strongest intensity at 2θ = 34.5 and 36.1^0. No additional peaks of CeO_2 phase were observed in CuCe and CuCe(U) samples. It indicated that the CeO_2 species could barely be detected by means of the XRD technique, even with the CeO_2 loading up to 4 wt.%; the CeO_2 phase was well-dispersed on the material. Based on the XRD result at the highest peak with 2θ = 36.1^0, the average size of crystals in the samples was determined based on the Scherrer's equation. The average crystal sizes of Cu(U), CuCe, and CuCe(U) catalysts were determined

as being 17.2, 15.7, and 14.5 nm, respectively. With CuCe and CuCe(U) samples, the CeO_2 species could barely be detected bythe XRD technique, which suggests that CeO_2 is well-dispersed.

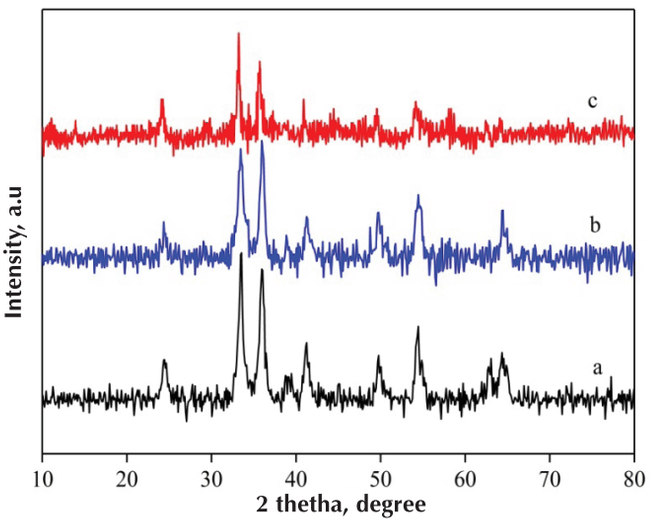

Fig. 1. XRD patterns of catalysts: a) Cu(U); b) CuCe; c) CuCe(U).

The SEM images illustrated that the catalysts reached high porosity with small nanoparticle size (illustrated in Fig. 2). The surface structure of all samples appeared to be more porous. Based on the TEM images of samples, one can deduce that the modification of CuO supported on ZRM by the CeO_2 promoter and the addition of urea in the solution of precursors resulted in reduced particle size and increased CuO dispersion on the material relative to the CuO and ZRM catalyst [9] (illustrated in Fig. 3).

Based on TEM images of samples from the ImageJ software, the nanosized distribution of the samples was depicted in Fig. 4. Base on the size distribution histogram, the nanoparticles on the catalysts had a size range smaller than 50 nm, and the average particle sizes of the Cu(U), CuCe, and CuCe(U) catalysts were determined as being 16.6, 15.4, and 14.7 nm, respectively. These results were consistent with those obatined from the XRD results (seen in Fig. 5), in which the CuCe(U) sample exhibited the smallest nanoparticles.

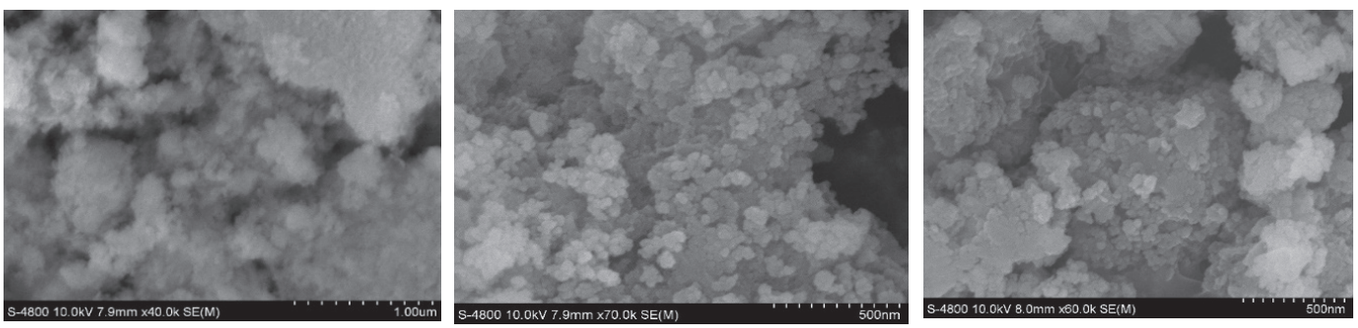

(A) Cu(U) **(B) CuCe** **(C) CuCe(U)**

Fig. 2. SEM images of catalysts.

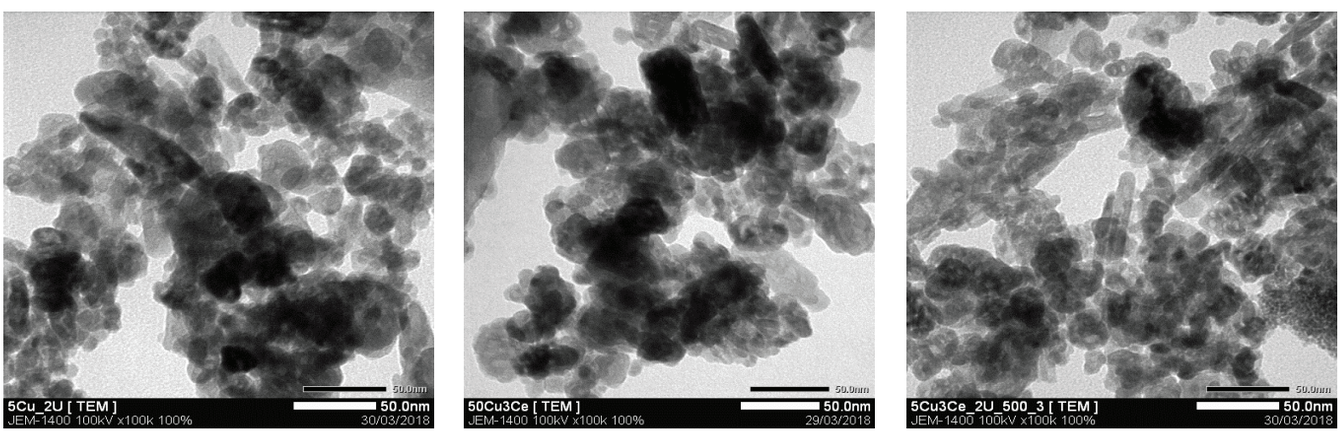

(A) Cu(U) **(B) CuCe** **(C) CuCe(U)**

Fig. 3. TEM images of catalysts.

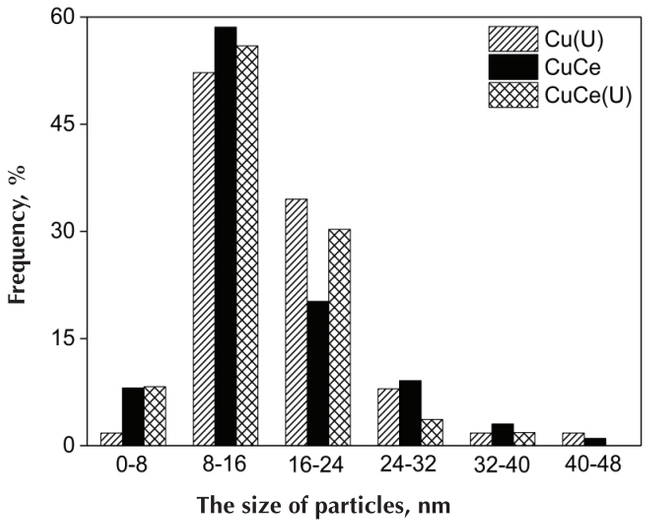

Fig. 4. Size distribution histogram of catalysts.

Comparisons of the BET specific surface area, average pore diameter, pore volume and particle size of the samples are illustrated in Fig. 5. The samples reached medium BET surface and porosity. Relative to CuCe and Cu(U), the CuCe(U) catalyst had a higher BET surface area (40 m^2/g) and a larger pore volume (0.027 m^3/g). The results demonstrated that the CuCe(U) sample exhibited higher porosity and smaller nanoparticles with higher reduction, which could result in an enhanced catalytic performance in BTX deep oxidation.

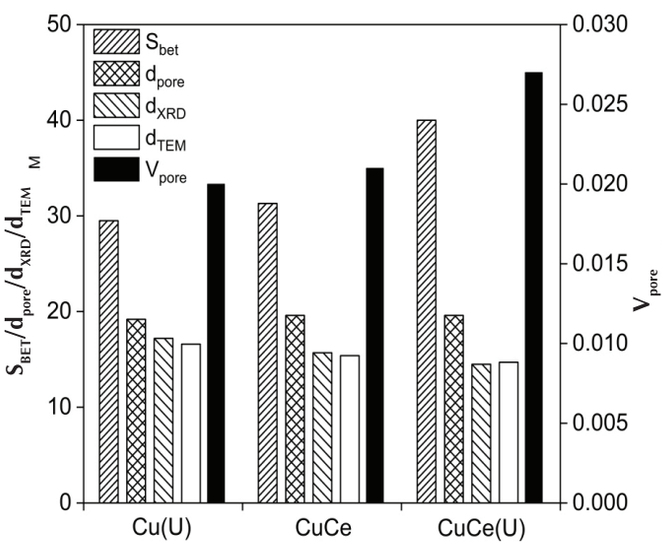

Fig. 5. Comparison of the BET surface (S_{BET}, m^2/g), average pore diameter (d_{pore}, Å), pore volume (V_{pore}, cm^3/g), and average diameter of particles based on the XRD results at 2θ = 36.1⁰ (d_{XRD}, nm) and the TEM results (d_{TEM}, nm) of samples.

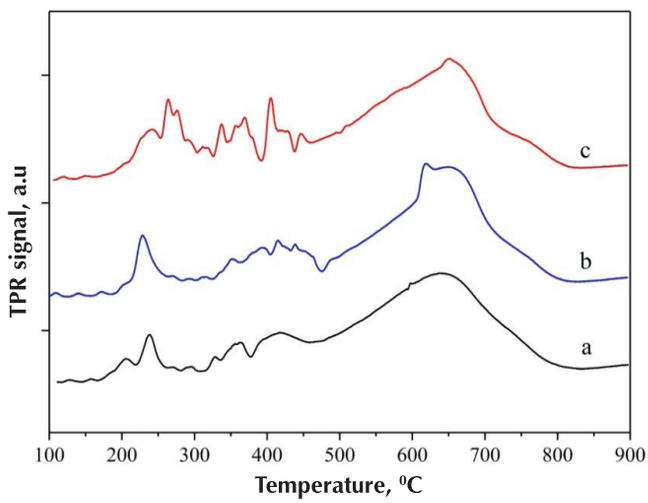

Fig. 6. TPR profiles of catalysts: (a) Cu(U); (b) CuCe; (c) CuCe(U).

The H_2-TPR patterns of samples are depicted in Fig. 6. The H_2-TPR profile of the CuCe sample displays three reduction peaks. The first peak at the temperature range of 200 to 300⁰C resulted from the reduction of the bulk-like CuO phases [11]; the second peak with a low intensity at the temperature range of 300 to 450⁰C was attributed to the reduction of Fe_2O_3 to Fe_3O_4; the third broad one at 450 to 850⁰C with T_{max} = 700⁰C could be ascribed to the reduction process from Fe_3O_4 to FeO or Fe [12]. On the CuCe and CuCe(U) samples, another peak at the range of 400 to 500⁰C was regarded as a characteristic of CuO bound to CeO_2. Relative to previous studies [9], the materials shifted to the lower temperature range; therefore, this catalyst was reduced more easily. In the CuCe(U) sample, the peak was narrower than another. This proved that CuO, CeO_2, and Fe_2O_3 had enhanced dispersion with smaller particle sizes in this sample.

Performance of the materials in the BTX treatment

Figure 7 illustrates the catalytic activity of the materials in terms of BTX oxidation. The conversion of p-xylene on all catalysts was higher than that of both benzene and toluene. Evidently, the catalytic activity of all samples increased in the following order: benzene < toluene < *p*-xylene. This consequence confirmed that the catalytic activity for the treatment of aromatic compounds is highly reliant upon the ionisation potential of methyl derivatives, the strength of the weakest C\H bond in the structure, and the relative adsorption strength of model compounds. All

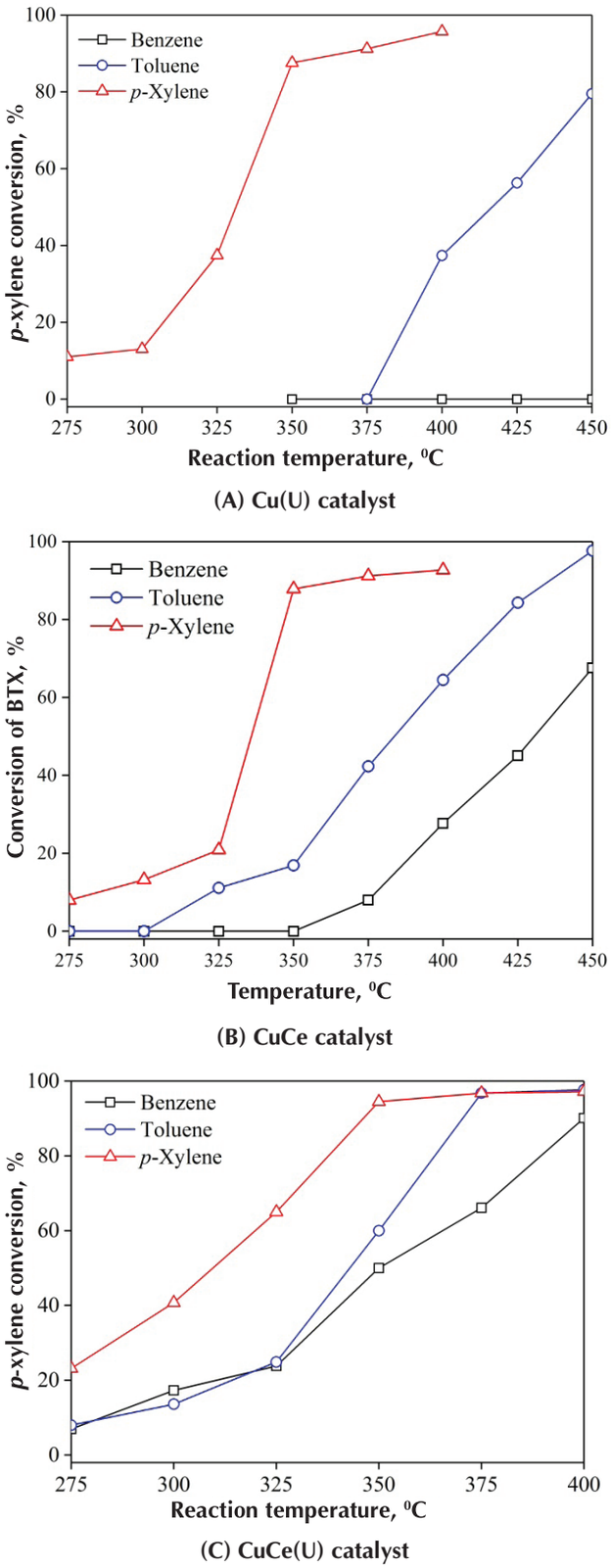

Fig. 7. The catalytic activity of samples in deep oxidation of benzene, toluene, and *p*-xylene (V = 12,000 ml.h^{-1}.g^{-1}; m_{cat} = 1.0 gam; C_{BTX}= 0.34 mol%; C_{oxy} = 10.5 mol%).

catalysts exhibited low activity at reaction temperatures below 300^{0}C. With further increasing reaction temperature, the catalysts became highly active performances, in which the complete conversion of *p*-xylene over all materials was obtained at the reaction temperature of 400^{0}C; it achieved complete conversion of toluene at 450^{0}C. This indicated that the highest BTX conversion was obtained by the CuCe(U) sample. It exhibited superior catalytic performance in terms of the conversions of *p*-xylene, toluene, and benzene, corresponding to 95, 60, and 55% at a reaction temperature of 350^{0}C.

Therefore, the modification of CuO and ZRM by the combination of the CeO_2 promoter and addition of urea to the solution of precursors resulted in reduced particle size, increased CuO dispersion on the material surface, and enhanced catalytic activity of the material. This was demonstrated by the XRD, SEM, TEM, BET, and H_2-TPR results.

Conclusions

Three catalysts prepared through wetness impregnation or the combustion method towards BTX deep oxidation have been evaluated. All samples demonstrated the small nanoparticle size, the high dispersion of copper and the ceria species, and the strong support of metal interaction, which presented more Ce^{4+}/Ce^{3+} and/or Cu^{2+}/Cu^{+} redox couples and indicated a high redox ability. The material synthesised through the combination of the CeO_2 promoter and the addition of urea to the solution of the precursors - CuCe(U) sample exhibited the optimal catalytic performance in terms of BTX oxidation. The catalytic activity of materials in the oxidation of BTX compounds is significantly impacted by the strength of the weak C\H bond in the structure of each BTX.

ACKNOWLEDGEMENTS

The study was supported by Science and Technology Incubator Youth Program, managed by the Center for Science and Technology Development, Ho Chi Minh Communist Youth Union, the contract number is "09/2018/HD-KHCN-VU".

The authors declare that there is no conflict of interest regarding the publication of this article.

REFERENCES

[1] M.S. Kamal, S.A. Razzak, M.M. Hossain (2016), "Catalytic oxidation of volatile organic compounds (VOCs) - a review", *Atmospheric Environment*, **140**, pp.117-134.

[2] A.J. Schwanke, S.B. Pergher, L.F. Probst, R. Balzer (2017), "Gallium-containing mesoporous silica: supported catalysts with high catalytic activity for oxidation of benzene, toluene and o-xylene", *Journal of the Brazilian Chemical Society*, **28(1)**, pp.42-48.

[3] W.A. da Costa, C.R. Lima, F.G.S. da Silva Filho, M.S. de Oliveira, R.M. Cordeiro, R.N. de Carvalho Junior, M.C. Martelli, D.D.S.B. Brasil (2017), "Computer simulation of benzene, toluene and p-xylene adsorption onto activated carbon", *African Journal of Biotechnology*, **16(20)**, pp.1176-1181.

[4] H.S. Kim, T.W. Kim, H.L. Koh, S.H. Lee, B.R. Min (2005), "Complete benzene oxidation over Pt-Pd bimetal catalyst supported on γ-alumina: influence of Pt-Pd ratio on the catalytic activity", *Applied Catalysis A: General*, **280(2)**, pp.125-131.

[5] Y. Liu, R. Naidu, H. Ming (2011), "Red mud as an amendment for pollutants in solid and liquid phases", *Geoderma*, **163(1-2)**, pp.1-12.

[6] D.T.N. Quyen, L.C. Loc, H.K.P. Ha, D.T.H. Nga, N. Tri, N.T.T. Van (2017), "Synthesis of adsorbent with zeolite structure from red mud and rice husk ash and its properties", *AIP Conference Proceedings*, p.020034.

[7] A. Huang, Y. Lin, W. Yang (2004), "Synthesis and properties of A-type zeolite membranes by secondary growth method with vacuum seeding", *Journal of Membrane Science*, **245(1-2)**, pp.41-51.

[8] S. Ordóñez, H. Sastre, F.V. Díez (2001), "Characterisation and deactivation studies of sulfided red mud used as catalyst for the hydrodechlorination of tetrachloroethylene", *Applied Catalysis B: Environmental*, **29(4)**, pp.263-273.

[9] D.T.M. Hieu, T.Q. Thinh, N. Tri, N.T.T. Van, H.K.P. Ha (2018), "Fabrication of CuO-doped catalytic nanomaterial containing zeolite synthesized from red mud and rice husk ash for CO oxidation", *Adv. Nat. Sci.: Nanosci. Nanotechnol.*, **9**, p.025005 (7pp).

[10] D. Volanti, D. Keyson, L. Cavalcante, A.Z. Simões, M. Joya, E. Longo, J.A. Varela, P. Pizani, A. Souza (2008), "Synthesis and characterization of CuO flower-nanostructure processing by a domestic hydrothermal microwave", *Journal of Alloys and Compounds*, **459(1)**, pp.537-542.

[11] C.L. Luu, T. Nguyen, T.C. Hoang, M.N. Hoang, C.A. Ha (2015), "The role of carriers in properties and performance of Pt-CuO nanocatalysts in low temperature oxidation of CO and p-xylene", *Adv. Nat. Sci.: Nanosci. Nanotechnol.*, **6**, p.015011 (9pp).

[12] S. Sushil, V.S. Batra (2008), "Catalytic applications of red mud, an aluminium industry waste: a review", *Applied Catalysis B: Environmental*, **81(1)**, pp.64-77.